Strain dependent facet stabilization in selective-area heteroepitaxial growth of GaN nanostructures

F. Shahedipour-Sandvik[a] and J. Grandusky
College of Nanoscale Science and Engineering, University at Albany-SUNY, Albany, New York 12203

A. Alizadeh,[a] C. Keimel, S. P. Ganti, S. T. Taylor, and S. F. LeBoeuf
General Electric, Global Research Center, Niskayuna, New York 12309

P. Sharma
Department of Mechanical Engineering, University of Houston, Houston, Texas 77204

(Received 28 February 2005; accepted 20 September 2005; published online 29 November 2005)

We report on the selective-area heteroepitaxy and facet evolution of submicron GaN islands on GaN-sapphire, AlN-sapphire, and bare sapphire substrates. It is shown that strain due to the lattice mismatch between GaN and the underlying substrate has a significant influence on the final morphology and faceting of submicron islands. Under identical metalorganic chemical vapor deposition growth parameters, islands with low or no mismatch strain exhibit pyramidal morphologies, while highly strained islands evolve into prismatic shapes. Furthermore, islands grown with relatively low compressive mismatch strain yield more uniform arrays of pyramids as compared to the nonstrained, homoepitaxially grown crystals. It is proposed that the strain dependency of Ehrlich-Schwoebel barriers across different crystallographic planes could potentially account for the observed morphologies during selective area growth of GaN islands. © *2005 American Institute of Physics*. [DOI: 10.1063/1.2131199]

The key to the realization of high performance nanoscale optoelectronic devices is the synthesis of tailored semiconductor nanostructures with precisely controlled position, size, composition, and shape. Selective area epitaxy (SAE) is perhaps one of the most promising routes for the fabrication of well-defined nanostructures, since it not only allows for control of size and location with nanoscale precision, but also avoids the nonradiative defects associated with the direct writing techniques.[1,2] SAE or templated growth of numerous materials with dimensions ranging from tens of nanometers to a few microns, has been reported in the literature.[3–6] Arrays of crystalline nanoisland geometries, have also been observed during SAE of GaN[7] and other compound semiconductors, sparking much interest in their possible use as cold cathode field emitters[8] and as optoelectronic components.[9]

The impact of crystal morphology and faceting on the optoelectronic properties, and potential device performance, of GaN structures (particularly, sub-100 nm GaN quantum dots and nanowires) is generally well established.[10,11] Facet stabilization during SAE of GaN nanostructures on GaN layers has been extensively investigated as a function of growth parameters.[7,12,13] In contrast, morphology evolution accompanying selective-area *heteroepitaxy* of wide band gap nanostructures has received less attention. Heteroepitaxial growth of GaN is commonly carried out on substrates such as sapphire with large lattice and thermal mismatch with respect to GaN. This, in turn, leads to highly strained films/islands, especially in the vicinity of the substrate interface. In this letter, we investigate the correlation between interfacial mismatch strain and facet evolution during SAE growth of GaN nanostructures on various lattice-mismatched substrates. Field emission scanning electron microscopy (FE-SEM) and transmission electron microscopy (TEM) are utilized in concert with theoretical models to correlate the observed morphology of submicron SAE GaN islands with predicted changes in the Ehrlich-Schwoebel (ES) barrier as a function of interfacial strain.

SAE was conducted on three different types of substrates: 3-μm-thick *c*-plane GaN on sapphire, 1-μm-thick *c*-plane AlN on *c*-plane sapphire; and bare *c*-plane sapphire substrate. A 100-nm-thick SiO_2 layer was deposited on each substrate by sputtering. Conventional UV lithography and reactive ion etching techniques were used to generate 700 nm diameter circular openings in the SiO_2 layer. GaN islands were grown in a D180 Veeco metalorganic chemical vapor deposition (MOCVD) system. The SAE of submicron GaN was performed at 1050 °C and 100 Torr using trimethylgallium (124 μmol/min) and ammonia (8 slm) as precursors. Growth time was varied between 0 and 300 s. We used FE-SEM and TEM to characterize the samples.

To gain insight into the growth at the initial stages, GaN nano-islands were grown on GaN and sapphire substrates for growth times ranging from 0 and 10 s. Subsequent to the introduction of alkyl precursors, small GaN nuclei (with dimensions of 10–20 nm) are uniformly deposited inside the mask. A rather similar behavior is observed for SAE on AlN substrate with a delay in GaN nucleation. Furthermore, fewer and larger nuclei of trapezoidal shape are formed at the edges of the SiO_2 mask on bare sapphire, with the longest delay in GaN nucleation initiation. This behavior in nucleation initiation and island formation can be understood in terms of the heteroepitaxial lattice misfit.[14]

At later stages of growth, lateral growth and coalescence of these islands are observed, regardless of the substrate.

[a]Authors to whom correspondence should be addressed; electronic mail: sshahedipour@uamail.albany.edu, alizadeh@research.ge.com

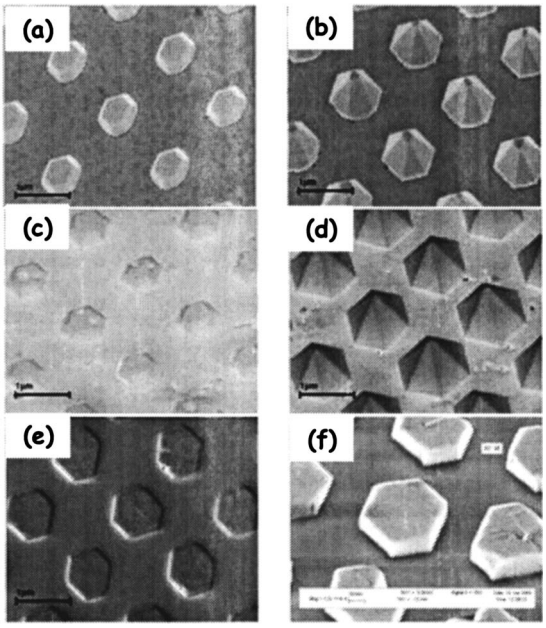

FIG. 1. Island growth and faceting of GaN on GaN/sapphire substrate after (a) 60 and (b) 180 s growth times; GaN on AlN/sapphire after (c) 90 and (d) 300 s growth times; and GaN on sapphire substrate after (e) 90 and (f) 180 s growth times.

In Figs. 1(a)–1(f), snapshots of island growth subsequent to coalescence are shown for the three substrates. As seen in Figs. 1(b) and 1(d), SAE on GaN and AlN result in hexagonal pyramidal shaped submicron islands. The facets of the pyramid were determined to belong to {1-101} family of planes.[15] For both GaN and AlN substrates, truncated pyramidal islands are clearly observed for growth times smaller than 120 s with highly uniform array of pyramids on AlN observed for longer than 300 s. SAE on highly lattice mismatched sapphire substrates results in the formation of prismatic GaN submicron islands.

The experimental work presented here highlights the importance of substrate material on facet evolution during submicron SAE. GaN islands experience different strain fields as a result of lattice mismatch with the underlying substrate. In the following, we attempt to explain our observations in the context of existing growth models and crystal faceting theories.

Hiramatsu *et al.* have systematically studied the effects of MOCVD process parameters on GaN crystal faceting during selective-area homoepitaxial growth.[9] These studies reveal that hexagonal pyramidal structures are the result of growth on rectangular and circular masks at relatively low temperatures, high pressures, and high precursor flow ratios. Under these conditions, due to reduced mobilities, adatom deposition rates are higher than their diffusion rates thus enhancing three-dimensional (3D) crystal formation. In addition, because of lower values of surface energies, {1-101} planes are more stable at these growth conditions. These studies also show that prismatic island formation is due to the enhanced adatom mobility as well as higher stability of the {0001} facet as compared to the {1-101} facet. Hiramatsu's phenomenological model, however, does not explain the influence of substrate induced strain on the faceting of the GaN islands during SAE.

Wulff's construction rule is the classical theory used to predict the equilibrium shape of a crystal by minimizing its total surface energy.[16] Recently, Muller and Kern have extended Wulff's and related theories to describe equilibrium crystal shapes in lattice-mismatched systems with coherent interfaces.[17] They conclude that strained crystals in the absence of interfacial misfit dislocations preferentially exhibit self-similar pyramidal shapes changing to crystals with flat top facets with dislocation generation. Our observation cannot be explained in the context of these models, since flat top crystals persist in heteroepitaxially grown GaN nanostrucutures, regardless of misfit dislocation density. One should note that Wulff construction rule is an equilibrium based theory whereas fully equilibrated structures under current MOCVD growth conditions are not expected.

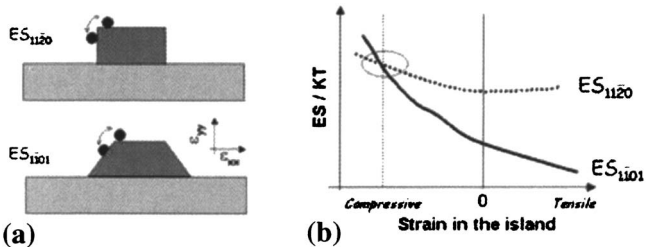

FIG. 2. (a) Schematic of Eherlich-Schowebel barriers and (b) their strain dependency in GaN islands.

Crystal morphology is ultimately governed by growth rates of various planes during adatom deposition and diffusion. It is well understood that the ES barrier renders the descent of atoms at step edges difficult.[18] The effect of ES barrier is to impede layer-by-layer [two-dimensional (2D)] growth, thus promoting 3D island formation. The magnitude of ES barrier varies among different materials systems and across different crystallographic planes. This barrier can be significantly higher than thermal fluctuations at elevated temperatures.

Recently, several authors have analyzed the effect of substrate strain on adatom binding energies and ES barriers for fcc metals, using tight binding potential calculations.[19,20] These results seem to indicate that compressive strain inhibits exchange diffusion at the edges, thus increasing the magnitude of ES barrier and promoting 3D island formation as a result. Conversely, tensile strain decreases the ES barrier, resulting in layer-by-layer 2D crystal formation. Systematic studies of ES barriers in semiconductors, in general, and the strain dependency of such barriers, in particular, are scarce. In this letter, we will use similar arguments as those in fcc metals to qualitatively describe the faceting behavior of GaN on different substrates in terms of ES barrier. We expect this qualitative comparison to be valid due to similar stacking of atoms in fcc and hcp lattices while ignoring the effects of polarity and the ionic character of the crystal.

In Fig. 2(a), the schematic of adatom diffusion across the {0001}-{1-101} and {0001}-{11-20} edges is shown. The barriers for adatom diffusion across these edges will be referred to as $ES_{\{1\bar{1}01\}}$ and $ES_{\{11\text{-}20\}}$. In Fig. 2(b), we show a hypothetical schematic for the strain dependency of these barriers. Here, we theorize that the lattice strain dependency of ES barriers in GaN is qualitatively similar to that of Ag and Pt previously reported in the literature.[21] As it can be observed in Fig. 2(b), for homoepitaxial growth (zero strain), $ES_{\{1\bar{1}01\}}$ is assumed to be smaller than $ES_{\{11\text{-}20\}}$, favoring pyramidal (3D) growth in accordance with the experimental observations. Here different strain dependencies for the $ES_{\{1\bar{1}01\}}$ and

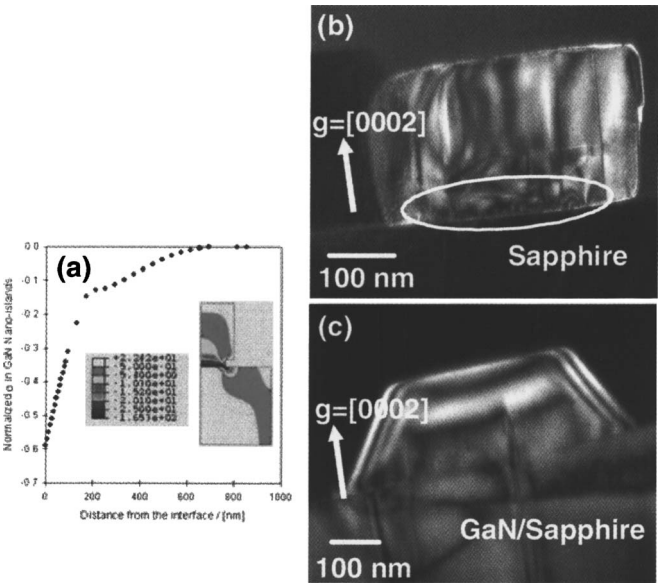

FIG. 3. (Color online) Stress distribution near the island/substrate interface. (a) FE calculations of stress contours and normalized in-plane stress in GaN on sapphire; normalization is with respect to the thin film case, 66.1 GPa for sapphire. Dark-field TEM images of (b) GaN island on sapphire and (c) GaN island on GaN/sapphire reveal differences in stress conditions near the island-substrate interface (white circle).

$ES_{\{11\text{-}20\}}$ barriers across various crystallographic planes has been assumed due to the variation of the effective normal strain across these different crystallographic facets.

Assuming that the $ES_{\{1\bar{1}01\}}$ and $ES_{\{11\text{-}20\}}$ exhibit strain dependencies similar to the schematic in Fig. 2(b), we can justify our current experimental observations as follows: For low to moderate compressive strains, an increase in both $ES_{\{1\bar{1}01\}}$ and $ES_{\{11\text{-}20\}}$ barriers severely impedes adatom diffusion to sidewalls. This in turn limits the extension of {0001} top facets, in accordance with the observation of highly sharp and regular GaN pyramids on AlN (2.7% compressive strain). On the other hand, for strains greater than a critical value [circled in Fig. 2(b)], the magnitude of $ES_{\{11\text{-}20\}}$ may become smaller than that of $ES_{\{1\bar{1}01\}}$. Therefore, adatom migration from the flat top surface to the perpendicular {11-20} sidewalls becomes energetically more favorable, promoting prismatic island formation.

While strain dependency of the ES barrier appears as a viable explanation for our physical observations, it does not address an important question: How far from the island/substrate interface is the effect of strain felt? To address this question, the finite element method[22] was employed to estimate the lattice mismatch induced stress/strain in these islands. Figure 3(a) shows the simulation results for normalized in-plane maximum compressive stress distribution in a prismatic GaN island on sapphire. Up to a distance of 600–800 nm from the island/substrate interface, the stress does not drop below 0.5 GPa. This high value of stress should have a significant effect on the ES barriers and surface energies of different crystal planes. At distances larger than 1 μm from the interface, the lattice misfit induced stresses drop significantly and hence crystal facet evolution should revert back to that of zero strain case. The presence of an unmitigated stress in a GaN island grown directly on sapphire can be seen in the cross-sectional TEM image of Fig. 3(b). This dark-field image reveals strain contours (circled) emanating from the island/substrate interface. For comparison, Fig. 3(c) shows an equivalent dark-field image of a GaN island grown on 3-μm-thick GaN on sapphire in which no strain contours can be seen at the interface.

In summary, we have established a plausible correlation between interfacial mismatch strain and facet evolution during selective area heteroepitaxial growth of GaN nanostructures on lattice-mismatched substrates. Under identical MOCVD growth parameters, islands with low or no mismatch strain exhibit pyramidal morphologies, while highly strained islands evolve into prismatic shapes. Facet control as a function of mismatch strain can be especially advantageous in circumstances where the growth-processing window for attaining high quality crystals is limited, such as MOCVD growth of high-quality ternary and quarternary nitride crystals.

Support from M. L. Blohm and the Nanotechnology Program at the GE Global Research Center are appreciated.

[1] Y. Xia, J. A. Rogers, E. P. Kateri, and G. M. Whitesides, Chem. Rev. (Washington, D.C.) **99**, 1823 (1999).
[2] Y. Arakawa, IEEE J. Sel. Top. Quantum Electron. **8**, 823 (2002).
[3] J. Y. Cheng, C. A. Ross, E. L. Thomas, H. I. Smith, and G. J. Vansco, Appl. Phys. Lett. **81**, 3657 (2002).
[4] S. C. Lee and S. R. Brueck, J. Appl. Phys. **96**, 1214 (2004).
[5] K. Tachibana, T. Someya, S. Ishida, and Y. Arakawa, J. Cryst. Growth **237**, 1312 (2002).
[6] K. Kawasaki, I. Nakamatsu, H. Hirayama, K. Tsutsui, and Y. Aoyagi, J. Cryst. Growth **243**, 129 (2002).
[7] T. Akasaka, Y. Kobayashi, S. Ando, N. Kobayashi, and M. Kumagai, J. Cryst. Growth **189/190**, 72 (1998).
[8] D. Kapolnek, R. D. Underwood, B. P. Keller, S. Keller, S. P. Denbaars, and U. K. Mishra, J. Cryst. Growth **170**, 340 (1997).
[9] K. Hiramatsu, J. Phys.: Condens. Matter **13**, 6961 (2001).
[10] T. Kuykendall, P. J. Pauzauskie, Y. Zhang, J. Goldberger, D. Sirbuly, J. Denlinger, and P. Yang, Nat. Mater. **3**, 524 (2004).
[11] A. Fonoberov, E. P. Pokatilov, and A. Balandin, J. Nanosci. Nanotechnol. **3**, 253 (2003).
[12] S. Kitamura, K. Hiramatsu, and N. Sawaki, Jpn. J. Appl. Phys., Part 2 **34**, L1184 (1995).
[13] K. Tachibana, T. Someya, I. Satomi, and Y. Arakawa, Appl. Phys. Lett. **76**, 3212 (2000).
[14] I. Daruka and A.-L. Barabasi, Phys. Rev. Lett. **79**, 3708 (1997).
[15] Z. Mao, S. McKernan, C. B. Carter, W. Yang, and S. A. McPherson, J. Cryst. Growth **204**, 270 (1999).
[16] G. Wulff, Z. Kristallogr. Mineral. **34**, 449 (1901).
[17] P. Muller and R. Kern, Surf. Sci. **457**, 229 (2000).
[18] S. J. Liu, H. Huang, and C. H. Woo, Appl. Phys. Lett. **80**, 3295 (2002), and references therein.
[19] B. Hinnemann, F. Westerhoff, and D. E. Wolf, Phase Transitions **75**, 151 (2002).
[20] B. D. Yu and M. Scheffler, Phys. Rev. B **56**, R15569 (1997).
[21] K.-H. hong, P.-L. Cha, and K.-K. Yoon, Mater. Sci. Forum **426–432**, 3463 (2003).
[22] A general purpose, commercially available finite element code, ABACUS, was used.